Numerical solution of the turbulent flow of an incompressible fluid in curved planar and axially symmetrical channels

I. Zuber*

The governing equations for axially symmetric flow, where the Reynolds stresses are expressed by scalar turbulent viscosity, are the Reynolds equations. The turbulence model k, ε is used in the well-known form for fully developed turbulent flow.

The numerical method, a continuation of the MAC system[1], is adapted so that even for high Reynolds cell numbers precision $0(\Delta x^2)$ can be achieved for the steady flow. Irregular cells join the rectangular network on the curved surface. Von Neumann's stability condition of the linearised numerical system is investigated. Special problems concerning the numerical solution of the turbulence model equations are stated and a special procedure is worked out to ensure that the fields k, ε do not converge to physically meaningless values. The program for the computer is universal in that the boundary problems can be assigned by input data.

As an example, an axially symmetrical diffuser with an area ratio of widening 1.40 is computed. Fields of velocity and pressure at the wall as well as fields ν_T and k are assessed. The results are compared with an experiment. The conclusion is that this method is suitable for the problems mentioned in this study as well as for unsteady flow

Key words: *turbulent flow, channel flow, incompressible flow*

During the last ten or fifteen years, considerable development of new methods in computational fluid dynamics has taken place. In spite of the rapid development of computing technology, it is still virtually impossible to cover the flow field by a sufficiently large number of discrete elements to describe all the details of turbulent flow. Thus, numerical treatments are still mere attempts at an optimal compromise to get results at a reasonable cost which can be used in practice with a certain precision and as a basis for further development. The progress of research in fluid dynamics has been hindered by numerous factors such as the present state of computing technology and the lack of both experimental and theoretical knowledge of turbulent flow.

Since the aims and means of the numerical treatment as well as the level of knowledge and the tradition of scientific work in various research institutes differ, the character of the optimal compromise mentioned above is also different. This is also why there is such a vast number of different numerical approaches.

* SVÚSS (National Research Institute for Machine Design), 250 97 Praha 9, Běchovice, Czechoslovakia
Accepted for publication 13 November 1981

The numerical procedure

The following conditions are considered:

- The computing technology is comparable to the IBM 360 as far as the operating speed is concerned and there is a ferrite-core memory of at least 512 kb;
- It is necessary to produce a universal program for various arbitrarily curved boundaries;
- As the Reynolds cell numbers are very high, it is impossible to use explicit methods with central differences;
- As the streamline usually deflects considerably from the direction of the coordinates, the UPWIND type systems are out of the question;
- As it is desirable to get some data about hydraulic losses, non-conservative methods are excluded;
- The next problem of interest is unsteady processes;
- The well known turbulence model k, ε adapted for fully developed turbulence with boundary conditions presupposing a logarithmic profile of the velocity near the wall is used;
- For the numerical treatment a rectangular network is used, completed by irregular cells near the curved wall. The MAC system[1] is combined with the system of Gourlay and Morris[2].

Basic equations

The following equations in the system of coordinates are taken as the basis of the numerical treatment:

 0142–727X/82/020091–09$03.00

$$\frac{\partial u}{\partial t}+\frac{\partial(u^2)}{\partial x}+\frac{1}{r}\frac{\partial(ruv)}{\partial r}$$
$$=-\frac{\partial p}{\partial x}+\frac{\partial \tau_{xx}}{\partial x}+\frac{1}{r}\frac{\partial(r\tau_{xr})}{\partial r} \quad (1)$$

$$\frac{\partial v}{\partial t}+\frac{\partial(uv)}{\partial x}+\frac{1}{r}\frac{\partial(rv^2)}{\partial r}$$
$$=-\frac{\partial p}{\partial r}+\frac{\partial \tau_{xr}}{\partial x}+\frac{1}{r}\frac{\partial(r\tau_{rr})}{\partial r}-\frac{\tau_{\varphi\varphi}}{r} \quad (2)$$

$$\frac{\partial u}{\partial x}+\frac{1}{r}\frac{\partial(rv)}{\partial r}=0 \quad (3)$$

where

$$\tau_{xx}=2\nu_T\frac{\partial u}{\partial x} \quad (4)$$

$$\tau_{xr}=\nu_T\left(\frac{\partial u}{\partial r}+\frac{\partial v}{\partial x}\right) \quad (5)$$

$$\tau_{rr}=2\nu_T\frac{\partial v}{\partial r} \quad (6)$$

$$\tau_{\varphi\varphi}=2\nu_T\frac{v}{r} \quad (7)$$

Variables u, v, p are time averaged values. The pressure p and the stresses are divided by the density ρ. The basic equations of the turbulence model are:

$$\frac{\partial k}{\partial t}+\frac{\partial(uk)}{\partial x}+\frac{1}{r}\frac{\partial(rvk)}{\partial r}$$
$$=\frac{\partial}{\partial x}\left(\frac{\nu_T}{\sigma_k}\frac{\partial k}{\partial x}\right)+\frac{1}{r}\frac{\partial}{\partial r}\left(\frac{\nu_T}{\sigma_k}r\frac{\partial k}{\partial r}\right)+\nu_T G-c_D\varepsilon \quad (8)$$

$$\frac{\partial \varepsilon}{\partial t}+\frac{\partial(u\varepsilon)}{\partial x}+\frac{1}{r}\frac{\partial(rv\varepsilon)}{\partial r}$$
$$=\frac{\partial}{\partial x}\left(\frac{\nu_T}{\sigma_\varepsilon}\frac{\partial \varepsilon}{\partial x}\right)+\frac{1}{r}\frac{\partial}{\partial r}\left(\frac{\nu_T}{\sigma_\varepsilon}r\frac{\partial \varepsilon}{\partial r}\right)+c_{3\varepsilon}kG-c_{2\varepsilon}\frac{\varepsilon^2}{k} \quad (9)$$

$$G=2\left(\frac{\partial u}{\partial x}\right)^2+\left(\frac{\partial u}{\partial r}+\frac{\partial v}{\partial x}\right)^2+2\left(\frac{\partial v}{\partial r}\right)^2 \quad (10)$$

$$\nu_T=\frac{k^2}{\varepsilon} \quad (11)$$

This system differs from the systems found in the literature in that the coefficient c_D is present in (8) instead of (11). The parameter ε used in the literature is equivalent to $c_D\varepsilon$ used here. The variable p includes an addition[5] of $\frac{2}{3}k$.

Boundary conditions are formulated at the distance y_c from the wall:

$$[u_c]_{y_c}=\frac{\tau^{1/2}}{\kappa}\ln\left(E\frac{y_c\tau^{1/2}}{\nu}\right) \quad (12)$$

$$[k]_{y_c}=\frac{\tau}{c_D^{1/2}} \quad (13)$$

$$[\varepsilon]_{y_c}=\frac{\tau^{3/2}}{\kappa c_D y_c} \quad (14)$$

A	Constant in (33)
BILH	Balance of the momentum of a little cell
c_1, c_2	Courant numbers
c_D, $c_{2\varepsilon}$, $c_{3\varepsilon}$	Constants of the turbulence model
d_1, d_2	Courant numbers divided by cell Reynolds numbers
E	Constant in (12)
DX, DR, DHX	Relative dimensions of special cells near the surface
f	Replaces u or v in (26)
G	Production of the turbulent energy divided by ν_T in (10)
FLX, FLR	Flux of momentum
k	Turbulent energy
L_x, L_r	Operators in (27) and (28)
KDE, KDK	Convective and diffusion term in (57) and (56)
p	Pressure divided by ρ
r	Coordinate
R_j	Distance of the axis
Re_c^1, Re_c^2	Cell Reynolds numbers
Rest	Residue
t	Time
u, v	Velocity in direction x, r
$\boldsymbol{u}$	Velocity vector
u_c	Velocity at the distance y_c from the wall, parallel with the wall
x	Coordinate
y_c	Thickness of the logarithmic region
Y_u, Y_v	Defined by (22)
Z	Source in (26)
Z_u, Z_v	Source (21)
γ	Auxiliary angle
ξ_t, ξ_1, ξ_2	Loss coefficients
ε	Turbulent energy dissipation divided by c_D
κ	Constant (~0.435)
ν_T	Turbulent viscosity
ν	Kinetic molecular viscosity
ρ	Density
σ_k, σ_ε	Constant of the turbulence model
τ	Stress at the wall divided by ρ
τ_{xx}, τ_{xr}, τ_{rr}, $\tau_{\varphi\varphi}$	Turbulent stresses divided by ρ
Φ_T	Dissipation integral (62)

Subscripts, superscripts and other symbols

ij	Subscripts for points in the network
n	Superscript for time level
Δx, Δr, Δt	Finite differences
$\vert_{App}^{ijn}$	Consistent approximation for points ij and time n

Subscripts in diagrams

d	Dynamic
m	Averaged with respect to the mass flux
s	Static
1, inl	Inlet
2, outl	Outlet

In (12), u_c is the velocity parallel to the wall and in the discrete system y_c is the distance of the p-point nearest to the wall.

The boundaries necessarily include the inlet and the outlet cross-sections, where heuristic conditions are used. At the inlet

$$u, v, k, \nu_T \text{ are given,} \quad \frac{\partial p}{\partial n} = 0 \tag{15}$$

At the outlet

$$\frac{\partial u}{\partial n}, \frac{\partial v}{\partial n}, \frac{\partial k}{\partial n}, \frac{\partial \nu_T}{\partial n} = 0 \tag{16}$$

$$p \text{ is given} \tag{17}$$

$\partial/\partial n$ indicates derivatives normal to the inlet or outlet cross-section. The values given at the inlet and outlet are related to the experiment, as it is always possible to get in the inlet section, to a certain extent, arbitrary values for u, v and to change the level of the turbulence k and ν_T, while the pressure across the outlet section is fairly constant.

The numerical method

This method makes use of the variables u, v, p, ν_T, k and ε to simulate the unsteady physical process. In the rectangular network, variables are located, according to the MAC system, as shown in Fig. 1.

Solution of the flow equations

The numerical solution determines $u_{i+\frac{1}{2}j}$, $v_{ij+\frac{1}{2}}$, p_{ij}. If velocity components with other subscripts eg u_{ij}, v_{ij} appear in the formulae, their values are taken as the average of the neighbouring values. The continuity equation is replaced by:

$$\left(\frac{\partial u}{\partial x} + \frac{1}{r}\frac{\partial (rv)}{\partial r}\right)\Bigg|_{\text{App}}^{ijn} = \frac{u_{i+\frac{1}{2}j} - u_{i-\frac{1}{2}j}}{\Delta x} + \frac{v_{ij+\frac{1}{2}} R_{j+\frac{1}{2}} - v_{ij-\frac{1}{2}} R_{j-\frac{1}{2}}}{R_j \, \Delta r} = 0 \tag{18}$$

In the following, the usual approximations according to the MAC system are used.

$$\frac{\partial p}{\partial x}\Bigg|_{\text{App}}^{i+\frac{1}{2}jn} = \frac{p^n_{i+1j} - p^n_{ij}}{\Delta x} \tag{19}$$

$$\frac{\partial u}{\partial t}\Bigg|_{\text{App}}^{i+\frac{1}{2}jn} = \frac{u^{n+1}_{i+\frac{1}{2}j} - u^n_{i+\frac{1}{2}j}}{\Delta t} \tag{20}$$

There are similar expressions for $\partial p/\partial r$ and $\partial v/\partial t$. Sources $Z^n_{u_{i+\frac{1}{2}j}}$ and $Z^n_{v_{ij+\frac{1}{2}}}$ are introduced including, contrary to the MAC system, the pressure term at time n resulting in:

$$Z^n_{u_{i+\frac{1}{2}j}} = \left(-\frac{\partial p}{\partial x} + \frac{\partial \tau_{xx}}{\partial x} + \frac{1}{r}\frac{\partial (r\tau_{xr})}{\partial r}\right)\Bigg|_{\text{App}}^{i+\frac{1}{2}jn} \tag{21}$$

A similar approximation is valid for $Z^n_{v_{ij+\frac{1}{2}}}$. Further, the quantity $Y_{u_{i+\frac{1}{2}j}}$ is introduced:

$$Y_{u_{i+\frac{1}{2}j}} = u^n_{i+\frac{1}{2}j} - \left(\frac{\partial (u^2)}{\partial x} + \frac{1}{r}\frac{\partial (ruv)}{\partial r}\right)\Bigg|_{\text{App}}^{i+\frac{1}{2}jn} \Delta t + Z^n_{u_{i+\frac{1}{2}j}} \, \Delta t \tag{22}$$

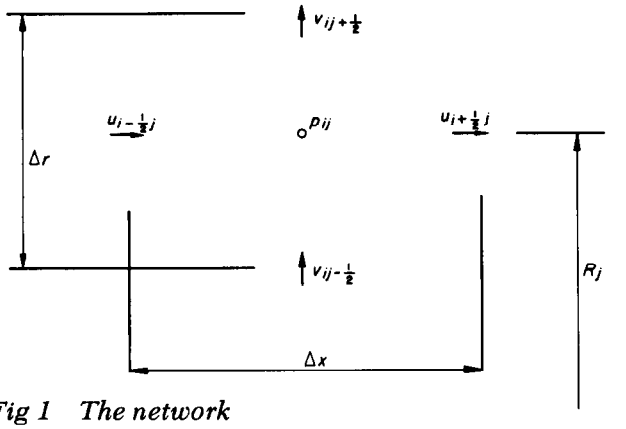

Fig 1 The network

Similar formulae are valid for $Y_{v_{ij+\frac{1}{2}}}$. Further, the quantity Δp_{ij} is introduced:

$$\Delta p_{ij} = p^{n+1}_{ij} - p^n_{ij} \tag{23}$$

Corresponding to the MAC system, new values of $u_{i+\frac{1}{2}j}$ and $v_{ij+\frac{1}{2}}$ are obtained for a pressure gradient at time $n+1$ such that the continuity equation at time step $n+1$ is satisfied. According to (22), with regard to (20), (21) and (23):

$$u^{n+1}_{i+\frac{1}{2}j} = Y_{u_{i+\frac{1}{2}j}} - \left(\frac{\partial}{\partial x}(\Delta p)\right)\Bigg|_{\text{App}}^{i+\frac{1}{2}j} \Delta t \tag{24}$$

and a similar expression is valid for $v^{n+1}_{ij+\frac{1}{2}}$. After insertion of (24) and the expression for $v^{n+1}_{ij+\frac{1}{2}}$ into the continuity equation at time $n+1$, an approximation of a Poisson equation for Δp_{ij} is achieved:

$$\left(\frac{\partial}{\partial x}\left(\frac{\partial (\Delta p)}{\partial x}\right) + \frac{1}{r}\frac{\partial}{\partial r}\left(r\frac{\partial (\Delta p)}{\partial r}\right)\right)\Bigg|_{\text{App}}^{ij} = \left(\left(\frac{\partial Y_u}{\partial x}\right)\Bigg|_{\text{App}}^{ij} + \left(\frac{1}{r}\frac{\partial (rY_v)}{\partial r}\right)\Bigg|_{\text{App}}^{ij}\right)\frac{1}{\Delta t} \tag{25}$$

The derivatives on the right side of (25) are expressed by the same difference approximation as the derivatives in the continuity equation. Because of this, the exact solution of the equations for Δp_{ij} provides the exact solution of the continuity equation at time step $n+1$. The term $1/\Delta t(\text{div } \boldsymbol{u})|_{\text{App}}^{ijn}$, providing the autoregulation of the continuity equation in the MAC system, is in this formulation included in the derivatives of Y_u and Y_v.

The solution procedure consists of three well-known phases:

1. Calculation of Y_u, Y_v
2. Calculation of the field Δp_{ij} by the ADI method
3. Calculation of $u^{n+1}_{i+\frac{1}{2}j}$, $v^{n+1}_{ij+\frac{1}{2}}$ (24)

The variables Y_u and Y_v are only outlined in (22); their precise formulation is given further on. Central differences cannot be used for high Reynolds cell-numbers, while UPWIND differencing is disregarded because of its large truncation error.

Introducing Δp in place of p permits the use of a variant of the Gourlay and Morris system[2] for the calculation of Y_u and Y_v. Formulae (22) for $Y_{u_{i+\frac{1}{2}j}}$ and the formulae for $Y_{v_{ij+\frac{1}{2}}}$ express a numerical solution of the following transport equation:

$$\frac{\partial f}{\partial t} = -\left(\frac{\partial (uf)}{\partial x} + \frac{1}{r}\frac{\partial (rvf)}{\partial r}\right) + Z \tag{26}$$

The symbol f stands for the component of momentum as an advected value while u and v represent the advective velocity field in (26).

In the Gourlay and Morris system[2] a promising numerical procedure is developed to solve similar equations. The full application is hindered by the fact that the source values are available only at time step n and therefore the source term must be properly worked into the numerical scheme.

The difference equation for the solution of (26) is written for points marked by subscripts ij where f is located. When the expression f_{ij}^{n+1} is used to formulate $Y_{u_{i+\frac{1}{2}j}}$ and $Y_{v_{ij+\frac{1}{2}}}$, half a spacing in the respective direction must be added. As in the MAC system, the advective field u and v is supposed to be constant in time interval Δt.

Operators of the Lax–Wendroff type are introduced:

$$L_x(f)_{ij} = f_{ij} - \frac{\partial(uf)}{\partial x}\bigg|_{\text{App}}^{ijn} \Delta t + \left(\frac{\partial}{\partial x}\left(u\frac{\partial(uf)}{\partial x}\right)\right)\bigg|_{\text{App}}^{ijn} \frac{\Delta t^2}{2} \tag{27}$$

$$L_r(f)_{ij} = f_{ij} - \left(\frac{1}{r}\frac{\partial(rvf)}{\partial r}\right)\bigg|_{\text{App}}^{ijn} \Delta t + \left(\frac{1}{r}\frac{\partial}{\partial r}\left(v\frac{\partial(rvf)}{\partial r}\right)\right)\bigg|_{\text{App}}^{ijn} \frac{\Delta t^2}{2} \tag{28}$$

These operators always solve one-dimensional equations without source with predictor in time $n+\frac{1}{2}$. In (27):

$$\frac{\partial(uf)}{\partial x}\bigg|_{\text{App}}^{ijn} = (u_{i+\frac{1}{2}j} f_{i+\frac{1}{2}j}^{n} - u_{i-\frac{1}{2}j} f_{i-\frac{1}{2}j}^{n})\frac{1}{\Delta x} \tag{29}$$

where

$$f_{i+\frac{1}{2}j} = (f_{i+1j} + f_{ij})\tfrac{1}{2} \tag{30}$$

and in the same equation,

$$\frac{\partial}{\partial x}\left(u\frac{\partial(uf)}{\partial x}\right)\bigg|_{\text{App}}^{ijn} = \left(u_{i+\frac{1}{2}j}\frac{\partial(uf)}{\partial x}\bigg|_{\text{App}}^{i+\frac{1}{2}jn} - u_{i-\frac{1}{2}j}\frac{\partial(uf)}{\partial x}\bigg|_{\text{App}}^{i-\frac{1}{2}jn}\right)\frac{1}{\Delta x} \tag{31}$$

The components of the advecting velocity $u_{i+\frac{1}{2}j}$ and $u_{i-\frac{1}{2}j}$ appear also in (29) and (31) which is why it is possible to rewrite $L_x(f)_{ij}$ in the form:

$$L_x(f)_{ij} = f_{ij} - (u_{i+\frac{1}{2}j} f_{i+\frac{1}{2}j}^{\text{red}} - u_{i-\frac{1}{2}j} f_{i-\frac{1}{2}j}^{\text{red}})\frac{\Delta t}{\Delta x} \tag{32}$$

Approximations in the operator $L_r(f)_{ij}$ are arranged similarly.

The solution of (26) is sought in the form:

$$f_{ij}^{n+1} = \tfrac{1}{2}(L_x(L_r(f)_{ij} + AZ_{ij}\,\Delta t)_{ij} + L_r(L_x(f)_{ij} + AZ_{ij}\,\Delta t)_{ij}) + (1-A)Z_{ij}\,\Delta t \tag{33}$$

It is also possible to rewrite the expression of f_{ij}^{n+1} into:

$$f_{ij}^{n+1} = f_{ij}^{n} - (u_{i+\frac{1}{2}j} f_{i+\frac{1}{2}j}^{\text{red}} - u_{i-\frac{1}{2}j} f_{i-\frac{1}{2}j}^{\text{red}})\frac{\Delta t}{\Delta x} - (v_{ij+\frac{1}{2}} f_{ij+\frac{1}{2}}^{\text{red}} R_{j+\frac{1}{2}} - v_{ij-\frac{1}{2}} f_{ij-\frac{1}{2}}^{\text{red}} R_{j-\frac{1}{2}})\frac{\Delta t}{R_j\,\Delta r} + Z\,\Delta t \tag{34}$$

The value of the symbol $f_{i+\frac{1}{2}j}^{\text{red}}$ in (34) is different from that of the identical symbol in (33). This form of transcription suggests that it is possible to express the result in such a way that the fluxes of momentum have the same value for the adjacent cells and this fact guarantees the conservative behaviour of the algorithm.

The quantity A in (33) makes possible the use of variants of the numerical method with $0 \leq A \leq 1$.

The precision of the approximation is usually assessed by the common method of replacing the discrete variables by Taylor series. The condition that the advective velocity field is time independent of the residue is given by:

$$Rest = \left(-\frac{\partial Z}{\partial t} + (1-A)\left(\frac{\partial}{\partial x}(uZ) + \frac{1}{r}\frac{\partial}{\partial r}(rvZ)\right)\right)\frac{\Delta t}{2} + 0(\Delta t^2) \tag{35}$$

As Δt is of the order $\Delta x/u_{\max}$, for $A = 1$ the differential approximation for the steady process is precisely $0(\Delta x^2)$. To ascertain the numerical stability, it is necessary to linearize (26). In doing this, it is important to keep in mind that the source Z includes in itself the friction (diffusion) term. Because of this, the stability of numerical solutions to the model equation (36) must be analysed:

$$\frac{\partial f}{\partial\left(\frac{t}{\Delta t}\right)} = -\left(c_1\frac{\partial f}{\partial\left(\frac{x}{\Delta x}\right)} + c_2\frac{\partial f}{\partial\left(\frac{y}{\Delta y}\right)}\right) + d_1\frac{\partial^2 f}{\partial\left(\frac{x}{\Delta x}\right)^2} + d_2\frac{\partial^2 f}{\partial\left(\frac{y}{\Delta y}\right)^2} \tag{36}$$

The variables in the model equation are quite common for analyses of this kind:

$$c_1 = \frac{u\,\Delta t}{\Delta x} \tag{37}$$

$$c_2 = \frac{v\,\Delta t}{\Delta y} \tag{38}$$

$$d_1 = \frac{c_1}{Re_c^1} = \frac{\nu_T\,\Delta t}{\Delta x^2} \tag{39}$$

$$d_2 = \frac{c_2}{Re_c^2} = \frac{\nu_T\,\Delta t}{\Delta y^2} \tag{40}$$

The dependence of the variables c_1 and c_2 on d_1 and d_2 for von Neumann's stability limit was achieved numerically and consequently $(c_1, c_2)_{\max}$ may be expressed as dependent on $\frac{1}{2}(d_1+d_2)$ and A according to Fig. 2.

From the stability tests (which will be mentioned again below) several values were plotted on the diagram. To assess Δt, the curves in the diagram were changed to broken lines. At each grid point the value M_{ij} was assessed as a function of γ and A, where:

$$\gamma = \arctan\left(\left(\frac{|u|}{\Delta x}, \frac{|v|}{\Delta y}\right)_{\max} \Big/ \frac{1}{2}\nu_T\left(\frac{1}{\Delta x^2} + \frac{1}{\Delta y^2}\right)\right) \tag{41}$$

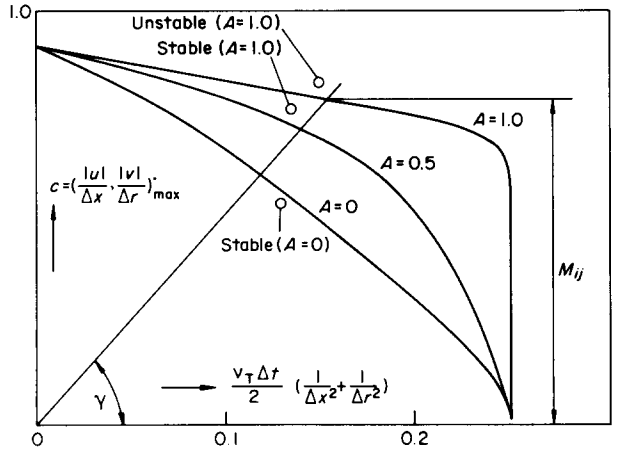

Fig 2 Stability of the linearised algorithm

In Fig. 2, M_{ij} is indicated for $A = 1$. At each point, the result is as follows:

$$\Delta t_{ij} = \frac{M_{ij}}{\left(\frac{|u_{ij}|}{\Delta x}, \frac{|v_{ij}|}{\Delta y}\right)_{\max}} \tag{42}$$

Δt was then determined as the least value of all the Δt_{ij} multiplied by k_t:

$$\Delta t = (\Delta t_{ij})_{\min} k_t \tag{43}$$

At the initial stage of the program development, $k_t = 0.8$ and $M_{ij} = 1$ were fixed which, however, for very high ν_T resulting from the turbulence model equations solution, led sometimes to instability and so it was necessary to assess Δt more precisely according to (41)–(43).

The following equations are used:

$$\begin{aligned} Y_{u_{i+\frac{1}{2}j}} = {} & \tfrac{1}{2}(L_x(L_r(u)_{i+\frac{1}{2}j} + AZ_{u_{i+\frac{1}{2}j}}\,\Delta t)_{i+\frac{1}{2}j} \\ & + L_r(L_x(u)_{i+\frac{1}{2}j} + AZ_{u_{i+\frac{1}{2}j}}\,\Delta t)_{i+\frac{1}{2}j}) \\ & + (1-A)Z_{u_{i+\frac{1}{2}j}}\,\Delta t) \end{aligned} \tag{44}$$

$$\begin{aligned} Y_{v_{ij+\frac{1}{2}}} = {} & \tfrac{1}{2}(L_x(L_r(v)_{ij+\frac{1}{2}} + AZ_{v_{ij+\frac{1}{2}}}\,\Delta t)_{ij+\frac{1}{2}} \\ & + L_r(L_x(v)_{ij+\frac{1}{2}} + AZ_{v_{ij+\frac{1}{2}}}\,\Delta t)_{ij+\frac{1}{2}} \\ & + (1-A)Z_{v_{ij+\frac{1}{2}}}\,\Delta t) \end{aligned} \tag{45}$$

All the terms of the source (except $\tau_{\varphi\varphi}$) may be expressed as the forces of friction and pressure acting on the elementary volume surface. The approximation for the pressure forces is given in (19) and at the inner points the forces of friction are as follows:

$$\tau_{xx}\Big|_{\text{App}}^{ijn} = \left(2\nu_T \frac{\partial u}{\partial x}\right)\Big|_{\text{App}}^{ijn} \tag{46}$$

$$\tau_{rr}\Big|_{\text{App}}^{ijn} = \left(2\nu_T \frac{\partial v}{\partial r}\right)\Big|^{ijn} \tag{47}$$

$$\tau_{xr}\Big|_{\text{App}}^{i+\frac{1}{2}j+\frac{1}{2}n} = \left(\nu_T\left(\frac{\partial u}{\partial r}+\frac{\partial v}{\partial x}\right)\right)\Big|_{\text{App}}^{i+\frac{1}{2}j+\frac{1}{2}n} \tag{48}$$

Specifying τ_{xx}, τ_{xr} and τ_{rr} at the cell boundaries guarantees the conservative behaviour of the algorithm. The assessment of the friction forces at the wall is based on the assumption that the friction force at the wall is given by:

$$\tau = \text{constant}\,(u^2 + v^2) \tag{49}$$

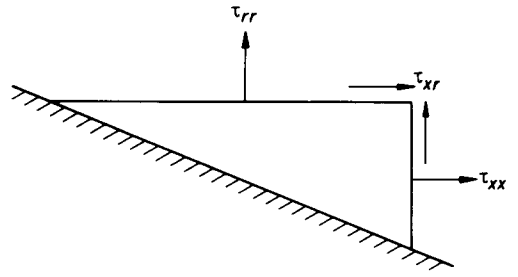

Fig 3 Stresses near the wall

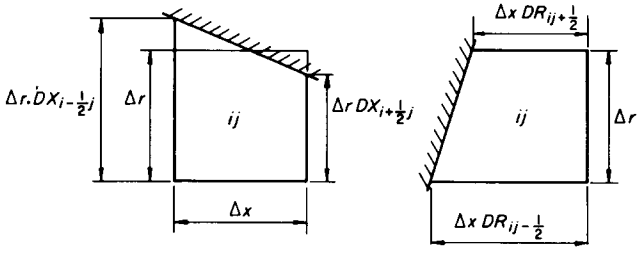

Fig 4 Cells for divergence

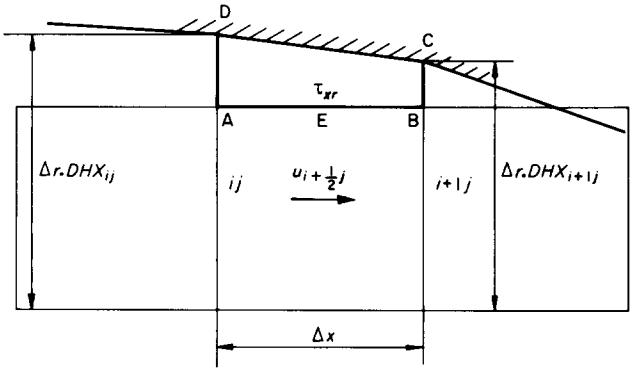

Fig 5 Cells for the momentum component

The constant is given in (12).

For arrangement according to Fig. 3:

$$\tau_{xr} = \text{constant}\,(u^2 - v^2) \tag{50}$$

$$\tau_{xx} = \tau_{xr} = -2\,\text{constant}\,uv \tag{51}$$

For u and v, the proximate averaged values are inserted.

Near the boundary the continuity equation is approximated by the following formulae:

$$\begin{aligned} \left(\frac{\partial u}{\partial x}+\frac{1}{r}\frac{\partial (rv)}{\partial r}\right)\Big|_{\text{App}}^{ij} = {} & \frac{u_{i+\frac{1}{2}j}DX_{i+\frac{1}{2}j} - u_{i-\frac{1}{2}j}DX_{i-\frac{1}{2}j}}{\Delta x} \\ & + \frac{v_{ij+\frac{1}{2}}DR_{ij+\frac{1}{2}}R_{j+\frac{1}{2}} - v_{ij-\frac{1}{2}}DR_{ij-\frac{1}{2}}R_{j-\frac{1}{2}}}{R_j\,\Delta r} \end{aligned} \tag{52}$$

Here $DX_{i+\frac{1}{2}j}$, $DR_{ij+\frac{1}{2}}$ indicate relative lengths and their meaning is given by Fig. 4. On the boundary, variables $DX_{i+\frac{1}{2}j}$ etc appear on both sides of (25).

The calculation of the balance of momentum near the wall is outlined in Fig. 5 for the x-component of momentum. First a preliminary momentum flux at the point E in Fig. 5 is fixed:

$$FLR_{i+\frac{1}{2}j+\frac{1}{2}} = u_{i+\frac{1}{2}j}v_{i+\frac{1}{2}j} \tag{53}$$

Preliminary values $Y^*_{u_{i+\frac{1}{2}j}}$ and $Y^*_{v_{ij+\frac{1}{2}}}$ are fixed with these values of momentum. On the boundary the balance of momentum of the cell A–B–C–D on Fig 5 is

$$\begin{aligned} BILH_{i+\frac{1}{2}j} = \frac{R_{j+\frac{1}{2}}}{R_j}(&FLR_{i+\frac{1}{2}j+\frac{1}{2}}\,\Delta x \\ &- FLX_{ij}(DHX_{ij}-1)\,\Delta r \\ &- FLX_{i+1j}(DHX_{i+1j}-1)\,\Delta r) \\ &+ (p_{ij}-p_{i+1j}) \\ &\times(\tfrac{1}{2}(DHX_{ij}+DHX_{i+1j})-1)\,\Delta r \end{aligned} \tag{54}$$

The surplus momentum $BILH$ is divided, according to the cross-sections of the little cell D–A, A–B, B–C as weighting coefficients among the adjoining cells. In Fig 5 this surplus is added to $Y^*_{u_{i-\frac{1}{2}j}}$, $Y^*_{u_{i+\frac{1}{2}j}}$, $Y^*_{u_{i+\frac{1}{2}j}}$ e.g.

$$\begin{aligned} Y_{u_{i-\frac{1}{2}j}} = Y^*_{u_{i-\frac{1}{2}j}} + &\left[\frac{BILH_{i+\frac{1}{2}j}\,\Delta t}{\Delta x\,\Delta r}\right] \\ &\times \frac{|(DHX_{ij}-1)|}{\Delta x + |(DHX_{ij}-1)|\,\Delta r + |(DHX_{i+1j}-1)|\,\Delta r} \end{aligned} \tag{55}$$

Solution of the turbulence model equations

If we compare the difficulties of the treatment of the flow equations and the turbulence model equations, there are both favourable and unfavourable conditions for the latter.

The favourable factors are:

1a) It is not necessary to strive for extreme accuracy, as the physical basis is only an approximation

2a) The approximations for the advective terms need not be very accurate, as these terms are usually small compared to the source terms.

The unfavourable factors are:

1b) The nonlinear source terms might cause instability

2b) The unsuitable choice of the initial fields of k and v_T might lead to instability or long computing time

3b) The coarse grid limits the value of the approximation of the source term $\nu_T G$ and makes the autoregulation of the difference system more difficult.

Let us briefly investigate the unfavourable factors. In principle, the discrete system can be written as:

$$k^{n+1} - k^n = KDK + \frac{k^2}{\varepsilon} G\,\Delta t - c_D \varepsilon\,\Delta t \tag{56}$$

$$\varepsilon^{n+1} - \varepsilon^n = KDE + c_{3\varepsilon} kG\,\Delta t - c_{2\varepsilon}\frac{\varepsilon^2}{k}\Delta t \tag{57}$$

In (56) and (57), the subscripts ij have been omitted. KDK and KDE are the sum of the advective and diffusive terms, which may be expressed as $a_1 - b_1 k$ and $a_2 - b_2 \varepsilon$ respectively, but for further considerations it is possible to take these terms as constant. The values k and ε on the right hand side may be substituted for time n or time $n+1$ or the mean value taken, eg $\frac{1}{2}(k^{n+1}+k^n)$.

Let us now evaluate the unfavourable factors in particular:

1b) Decrease of ε causes increase of k, but increase of k causes increase of ε. We must make sure that this process does not lead to instability.

2b) For low initial values of ε the increase of k will occasionally take a relatively long time, while the values of ν_T might be very high, hence the complicated calculation of Δt with (41)–(43).

3b) Difficulties may occur at the point of confluence of two streams. In the system of the differential equations the velocity gradient will increase considerably at such a point, which will cause the increase of G in (8) and (9) and, therefore, will also increase ν_T. The increase of ν_T will lead to a diminution of the velocity gradient. This is the background of the autoregulation of the system governed by partial differential equations. In the discrete system the increase of G in the coarse grid is limited roughly by the value $u^2_{max}/\Delta x^2$ and for low initial values of ν_T an unreal decrease of k may occur.

4b) If k, ε on the right hand side of (56), (57) are replaced by k^{n+1}, ε^{n+1} or $\frac{1}{2}(k^{n+1}+k^n)$, $\frac{1}{2}(\varepsilon^{n+1}+\varepsilon^n)$, it is possible to derive an algebraic equation of the 3rd degree for the ratio $\varepsilon^{n+1}/k^{n+1}$ or $(\varepsilon^{n+1}+\varepsilon^n)/(k^{n+1}+k^n)$. One of its real roots is negative and for sufficiently low Δt there are two other real roots, only one of which is physically meaningful.

The procedure is based on the following principles:

1. In the inlet cross-section, the fluctuation energy k and also ν_T are given by physical conditions. In the inner section of the integration area the initial ν_T field is guessed, roughly (0.05 to 0.1) $\Delta x u_{inl}$, and the initial field k is chosen in such a way that production and dissipation of the turbulent energy are balanced. In this way large oscillations of the k and ε values are prevented.

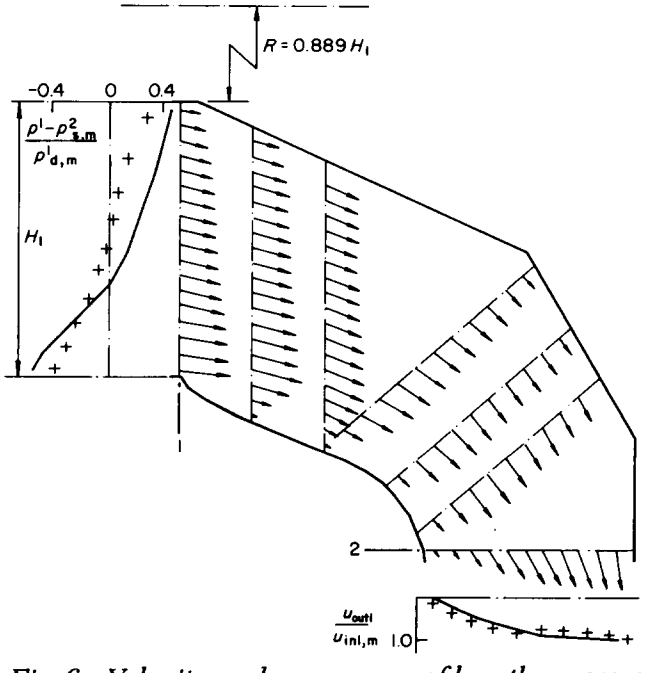

Fig 6 Velocity and pressure profiles, the crosses indicate experimental values

2. The convective term is written in a non-conservative form with an adapted UPWIND formula[6]. The approximation is of the type

$$-\left(u\frac{\partial k}{\partial x}+v\frac{\partial k}{\partial r}\right)$$

$$=\begin{cases}(k_{-v}-k^{n+1})\dfrac{|u|}{\Delta x} & \text{for } \dfrac{|u|}{\Delta x}>\dfrac{|v|}{\Delta r}\\[2ex](k_{-v}-k^{n+1})\dfrac{|v|}{\Delta r} & \text{for } \dfrac{|u|}{\Delta x}<\dfrac{|v|}{\Delta r}\end{cases} \tag{58}$$

We use the formula

$$u\frac{\partial k}{\partial x}+v\frac{\partial k}{\partial r}=(u^2+v^2)^{1/2}\frac{\partial k}{\partial s} \tag{59}$$

If k_v is a value interpolated on the streamline by a quadratic formula at a distance Δs upstream, then

$$\begin{aligned}(u^2+v^2)^{1/2}\frac{\partial k}{\partial s}\bigg|_{\text{App}} &= \frac{k_{ij}-k_{-v}}{\Delta s}(u^2+v^2)^{1/2}\\ &= (k_{ij}-k_{-v})\frac{|u|}{\Delta x}\\ &= (k_{ij}-k_{-v})\frac{|v|}{\Delta r}\end{aligned} \tag{60}$$

The truncation error is not dependent on the angle arctan (u/v) as in the case of the classic UPSTREAM approximation.

3. The diffusion term is written in a difference approximation of the type:

$$\left(\frac{\partial}{\partial x}\left(\nu_T\frac{\partial k}{\partial x}\right)+\frac{1}{r}\frac{\partial}{\partial r}\left(\nu_T\frac{\partial(rk)}{\partial r}\right)\right)\bigg|^{ij}_{\text{App}} = a-bk_{ij}^{n+1} \tag{61}$$

Here a and b contain the values of k, ν_T and ε at time level n.

4. Values for k and ε on the right hand sides of (56) and (57) are inserted at time $n+1$ and the system is rewritten into an algebraic equation of the 3rd degree for the ratio $\varepsilon^{n+1}/k^{n+1}$. The equation is solved by iteration, so that the larger positive root is obtained. If the equation has no positive real roots, the time step Δt is reduced at this point.

The computer program

The program in FORTRAN allows the user to specify the geometry of the problem by the input data without changing the program. To each point of the grid a certain code number is attached, indicating whether it is an inner point, a point close to the wall or a point of the inlet or outlet etc. The special dimensions of the little cells are also given by input data.

It is possible to choose the distance of the axis from the coordinate system, the number of the grid points, the ratio $\Delta r/\Delta x$, the turbulent model constants, the value A in (33), the safety factor k_t in (42) etc. The program makes use of nondimensional variables, the reference length is the spacing Δx; the reference velocity may be, in theory, chosen arbitrarily. It is however advisable, regarding the FORMAT of the print, to choose the reference velocity to be of the same order as the mean velocity.

The initial fields of u and v given by input data need not satisfy the continuity equation and the initial field for p is usually taken as zero. The initial fields of k and ν_T are also given by input data, but the program maintains the k values only on the inlet cross section and, for the remaining part, the k field is modified so that production and dissipation are balanced. The initial field ε is defined by k^2/ν_T.

The program verifies the conservation of momentum for the whole integration area and an error on the balance indicates incorrect input data characterising the geometry.

The program also includes calculation of the dissipation integral of the time averaged velocity field and enables computing of the energy balance:

$$\phi_T=\left(\int_v \nu_T\left(2\left(\frac{\partial u}{\partial x}\right)^2+\left(\frac{\partial u}{\partial r}+\frac{\partial v}{\partial x}\right)^2+2\left(\frac{\partial v}{\partial r}\right)^2\right)dv\right)\bigg|_{\text{App}} \tag{62}$$

The following choices of the computing procedure are made possible by this program:

1. Both the turbulent model and the prescribed time constant ν_T field may be used; the stresses on the walls may be calculated by turbulent or laminar formulae.

2. It is possible to transfer a set of values of u, v, p in each time step and in this way simulate the periodic boundary conditions in space.

3. It is possible to include a subroutine simulating a time variable velocity field in the inlet cross-section.

Application of the method

To demonstrate its application, an example of theoretical treatment of an axially symmetric diffuser with an area ratio of 1.40 is presented. The properties of such diffusers influence the losses of the casing of turbines; much attention has been given to these recently, (see for example Ref 8). The diffuser in question is outlined in Fig 6. The most specific feature of its geometry is the sudden partial widening just past the inlet.

In the experiments simulated by the numerical solution the turbulence in the inlet cross-section was artificially increased up to approximately 13%. The profile of the turbulence at the outlet has not been measured. The velocities and pressure both at the inlet and outlet and the pressure at the walls were measured in the experiments. The inlet velocity was about 50 m/s.

In the theoretical treatment, the casing contour was placed in a network of 32×28 points. There were 18 spacings Δr in the inlet, the ratio being $\Delta r/\Delta x=0.814$. The velocity field of the experiment was specified at the inlet; the level of the turbulent energy was also given there. The profile of k was assumed to be proportional to the square of the inlet velocity. As ν_T at the inlet was not given, the production and dissipation of the fluctuation energy in the inlet were assumed to be equal except for the point of the zero velocity gradient, where the proximate value was simply inserted. At the outlet cross-section the nearly uniform pressure profile was inserted according to the experiment.

A rough estimate of the initial velocity field was made regardless of whether it satisfied the continuity equation; the local violations of the continuity equation in the initial field were of the order $u_{max}/\Delta x$. The local deviations of the initial velocity from the resulting one amounted to 60% in relation to the mean inlet velocity, the safety coefficient in (43) was 0.95, for the constant A in (33) a value 1.0 was given and because of this, the method was formally exact $0(\Delta x^2)$ for the steady case. It took 300 time steps until the velocities were altered in successive time steps by less than 0.01% of the inlet velocity. In Fig. 6, velocity profiles are drawn in several cross-sections; the figure also shows the calculated inlet static pressure and calculated outlet velocity profile.

Fig 7 presents a comparison of the calculated pressures at the wall with the measured values. The theoretical values at the inner wall are very close to the experimental data, while at the outer wall the theory does not show the experimental decrease of the pressure near the sudden widening of the diffuser.

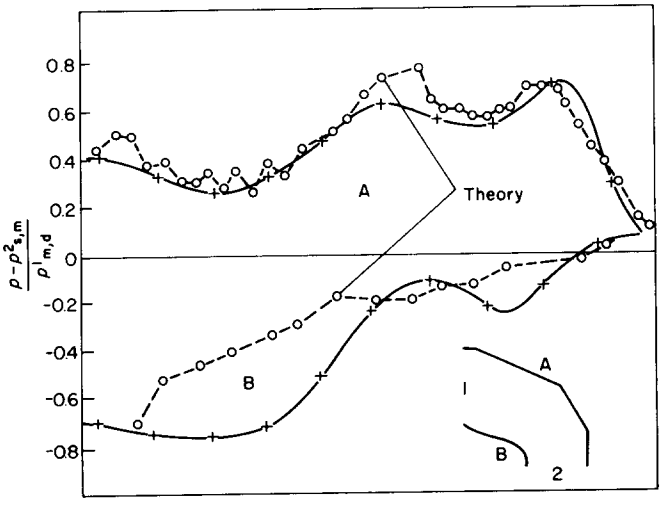

Fig 7 Pressures at the inner wall A and the outer wall B, the crosses indicate the experimental values

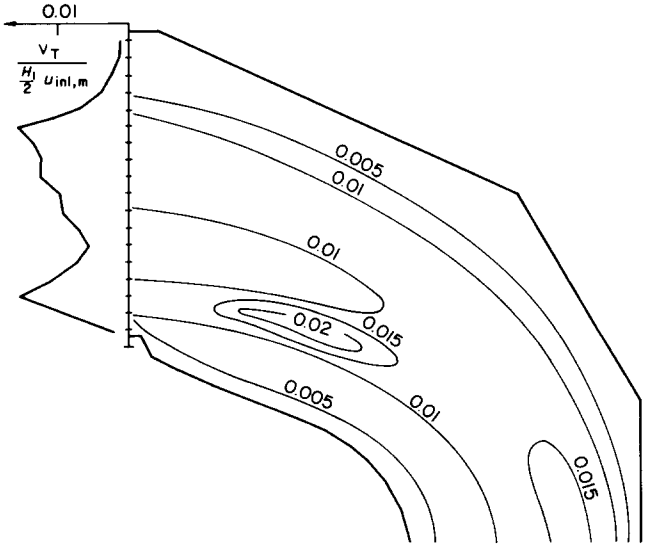

Fig 8 Field ν_T according to the turbulence model

Figs 8 and 9 show fields ν_T and k according to the turbulence model k, ε. Near the separation point, the values of k are considerably higher at the outer side; however, the ν_T values are only twice as large as those at the inner side. In Fig 10, the total pressure at the inlet and the outlet are compared for the same streamline. The diagram shows the theoretical and experimental profiles. According to the experiment, the total pressure on the streamline increases slowly near the inner wall. This increase is due to energy transport across the streamlines as a result of turbulent friction. If this small increase of energy on the streamline is neglected, the flow in the half of the channel nearer the inner wall is nearly a potential flow. In the part of the channel nearer the outer wall where the major part of dissipation of the time averaged flow takes place, this energy is being transformed into turbulence fluctuation energy. The theoretical solution is very instructive for the flow situations in this type of diffuser as follows from the total pressure profiles.

From the theoretical solution, loss coefficients have been derived. Since the numerical system does not conserve mechanical energy exactly, the integral (62) has been used for calculation of the energy dissipation of the time averaged flow. According to common usage, three kinds of loss coefficients have been used, indicating the losses in relation to the inlet kinetic energy. Coefficient ξ_t presupposes that all the kinetic energy in the outlet section is utilised, this coefficient being the measure of the dissipated energy. The other two coefficients are technological characteristics and it is considered that only a part of the kinetic energy in the outlet is utilised in the casing around the diffuser. ξ_1 presupposes that all the outlet kinetic energy is lost and ξ_2 that the kinetic energy of the mean outlet velocity is utilised.

In Table 1, the experimental and theoretical values of ξ_t, ξ_1 and ξ_2 are given.

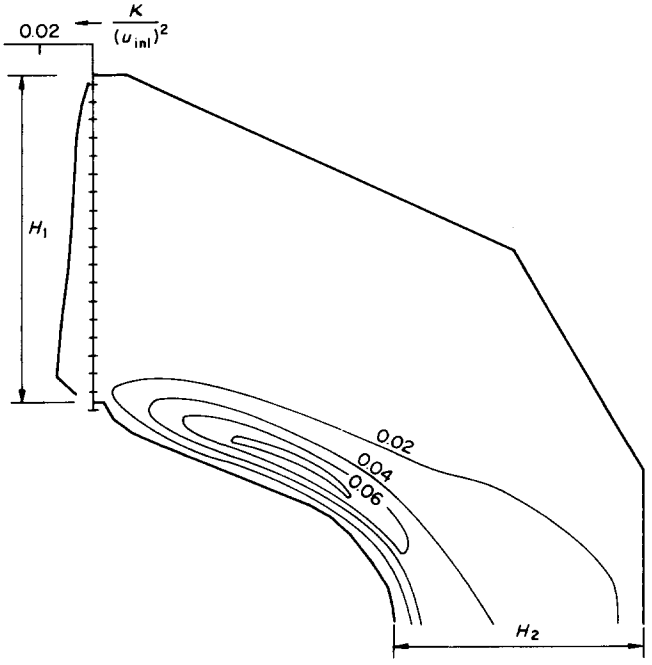

Fig 9 Field k according to the turbulence model

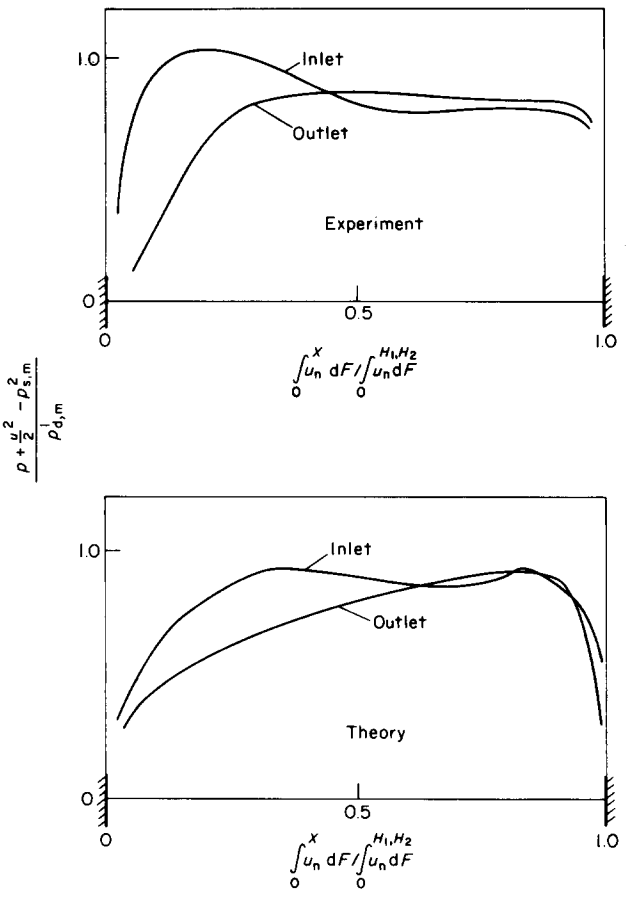

Fig 10 The total pressures at the inlet and outlet according to the experiment (top) and theory (bottom)

In the theoretical solution particularly, the coefficients ξ_1, ξ_2 (and probably also in the real case) depend to a high degree on the inlet velocity, k and ν_T field.

As an alternative, the coefficient ξ_t has been calculated from the total pressure balance, for the sake of control. The value $\xi_t = 0.148$ is closer to the measured value than the $\xi_t = 0.108$ obtained from the dissipation integral. All the same, the latter must be regarded as the more correct theoretical value and the difference $0.148 - 0.108 = 0.04$ must be taken as a coefficient characteristic of additional numerical dissipation of the discrete system.

The stability condition has also been tested. The system was unstable for $k_t = 1.05$ and stable for $k_t = 0.95$ with $A = 0.0$.

In solving the flow equations, it takes about 45% of the computing time to solve the Poisson equation. Five time steps of the system k, ε take about 80% of the computing time to solve the flow equations.

Table 1 Experimental and theoretical values of the loss coefficients

	ξ_t	ξ_1	ξ_2
Experiment	0.139	0.925	0.377
Theory	0.108	0.922	0.437

This methodology is also suitable for unsteady flow conditions, although for $A = 1$ the method is formally precise only to $0(\Delta t)$ in the unsteady case. The precision of the derivatives in time is only slightly less as the advective terms are evaluated using the predictor at time $n + \frac{1}{2}$. Results of the solution of flow around an isolated profile in a channel are given elsewhere[7], where periodically separated Karman's vortices have been illustrated by way of calculation.

Conclusion

A precise method has been developed, replacing the system of axially symmetric Reynolds equations and the turbulence model k, ε by a discrete system. The numerical method is precise $0(\Delta x^2)$ for steady flow and stable for Courant numbers near to one. The program is universal and it is suitable for solution of the flow in channels with curved surfaces. The solution for the axially symmetric diffuser provides a very realistic picture of the real flow conditions.

References

1. **Harlow F. H. and Welch J. E.** Numerical calculation of time-dependent viscous incompressible flow of fluid with free surface. *Physics of Fluids, 1965*, **9**, *104*
2. **Gourley A. R. and Morris J. L.** A multistep formulation of the optimized Lax–Wendroff Method for non-linear hyperbolic systems in two space variables. *Mathematics of Computation, 1968*, **22**(104), *715*
3. **Le Feuvre R. F.** Laminar and turbulent forced convection processes through in-line tube banks. *Imp. Coll. Mech. Eng. Dept. Tech. Note HTS/75*
4. **Stephenson P. L.** A theoretical study of heat transfer in two-dimensional turbulent flow in a circular pipe and between parallel and diverging plates. *Int. J. Heat & Mass Transfer, 1976*, **19**, *413*
5. **Hinze J. O.** Turbulence. *McGraw-Hill Book Company, New York, Toronto, London, 1959*
6. **Zuber I.** Ein mathematisches Modell des Brennraums. *Monographs and Memoranda No. 12, SVÚSS, Prague, 1976*
7. **Zuber I.** Application of finite difference method to two-dimensional turbulent unsteady flow. Strojirenstvi, *1979*, **29**(1), *25–31 (in Czech)*
8. **Šťastný M. and Feistauer M.** Flow in an annular axial-radial diffuser. *ASME-paper-78-GT-133*